Обзор ArXiv: astro-ph, 7-10 ноября 2017 года

От Сильченко О.К.

Astro-ph: 1711.00915

Star formation is boosted (and quenched) from the inside out: radial star formation profiles from MaNGA.

Sara L. Ellison[1], Sebastian F. Sánchez[2], Hector Ibarra-Medel[2], Braulio Antonio[1,2], J. Trevor Mendel[3], Jorge Barrera-Ballesteros[4]

[1] *Department of Physics & Astronomy, University of Victoria, Finnerty Road, Victoria, British Columbia, V8P 1A1, Canada.*
[2] *Instituto de Astronoma, Universidad Nacional Autonoma de Mexico, A. P. 70-264, C.P. 04510, Mexico, D.F., Mexico.*
[3] *Max-Planck-Institut fur Extraterrestrische Physik, Giessenbachstrasse, D-85748 Garching, Germany.*
[4] *Department of Physics & Astronomy, Johns Hopkins University, Bloomberg Center, 3400 N. Charles St., Baltimore, MD 21218, USA.*

6 November 2017

ABSTRACT

The tight correlation between total galaxy stellar mass and star formation rate (SFR) has become known as the star forming main sequence. Using ~ 487,000 spaxels from galaxies observed as part of the Sloan Digital Sky Survey Mapping Galaxies at Apache Point Observatory (MaNGA) survey, we confirm previous results that a correlation also exists between the surface densities of star formation (Σ_{SFR}) and stellar mass ($\Sigma_{\star}$) on kpc scales, representing a 'resolved' main sequence. Using a new metric ($\Delta\Sigma_{SFR}$), which measures the relative enhancement or deficit of star formation on a spaxel-by-spaxel basis relative to the resolved main sequence, we investigate the SFR profiles of 864 galaxies as a function of their position

В выборке почти поровну SF и пассивных галактик (по измерениям SDSS)

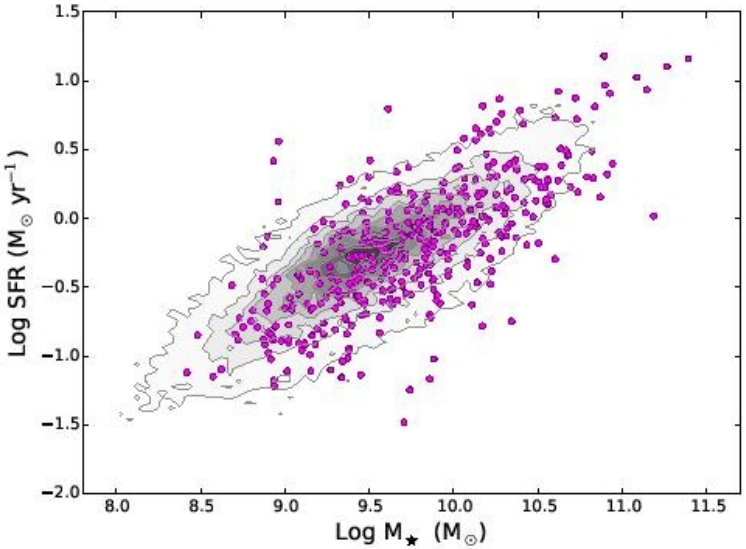

Figure 1. The star forming main sequence as defined by ~ 65,000 z<0.06 star forming galaxies from the SDSS DR7 (grey contours). Magenta points show the positions of 394 star forming MaNGA galaxies selected with the same criteria. Whilst all 394 galaxies are shown here for reference, two galaxies with $\Delta SFR < -1.0$ are transferred from the final star forming sample into the passive sample.

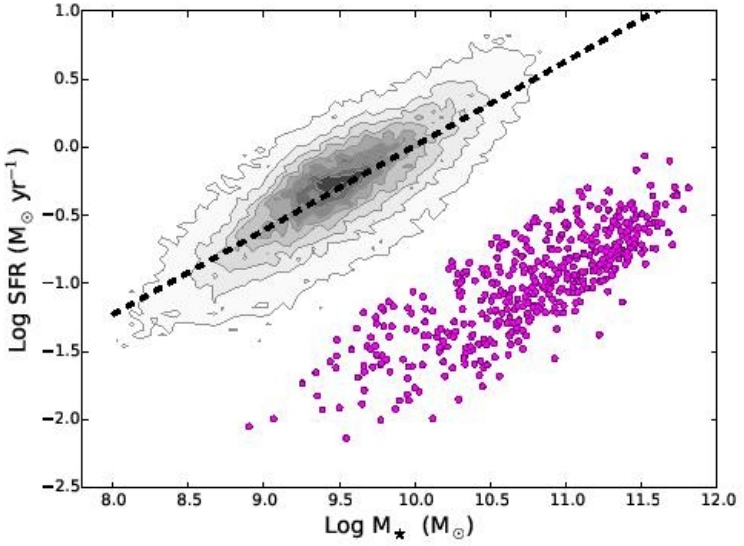

Figure 3. The star forming main sequence as defined by ~ 65,000 $z < 0.06$ star forming galaxies from the SDSS DR7 (grey contours). Magenta points show the positions of 470 MaNGA galaxies whose SFRs are at least a factor of 10 below the best fit (dashed line) through the main sequence and hence defined as passive.

А вот это уже главная последовательность и зависимость масса-металличность для элементов

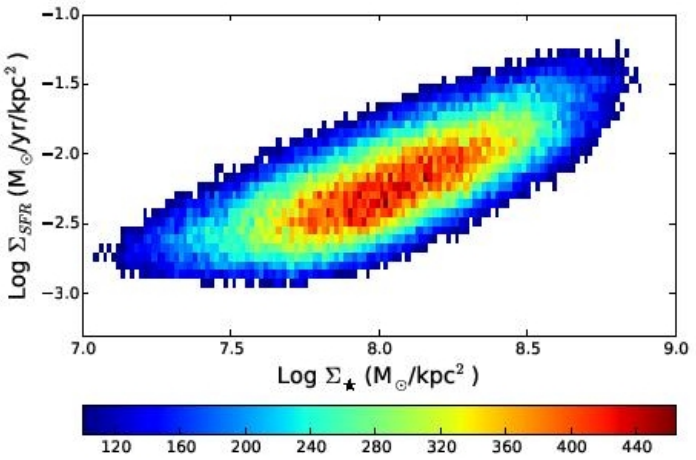

Figure 4. The local ('resolved') star forming main sequence for ~487,000 star-forming spaxels in the MaNGA DR13 datacubes. The colour bar indicates the number of spaxels in each bin. The minimum Σ_{SFR} is set by our definition of the star forming spaxel sample.

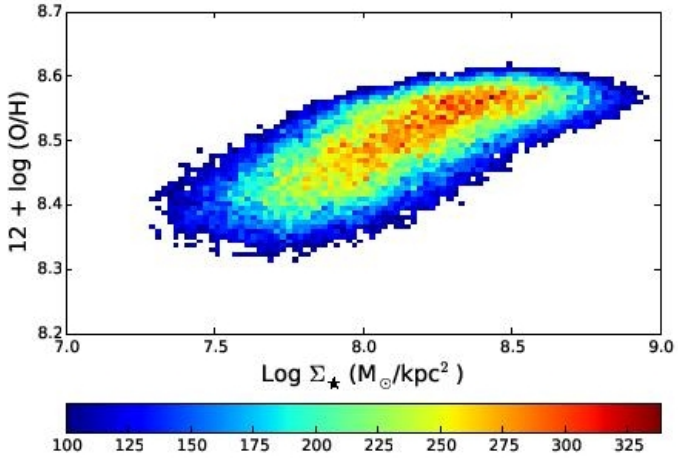

Figure 7. The local ('resolved') mass metallicity relation for ~487,000 star-forming spaxels in the MaNGA DR13 datacubes. The colour bar indicates the number of spaxels in each bin.

Темпы SF - по H-alpha и D4000

У пассивных подавлен именно центр!

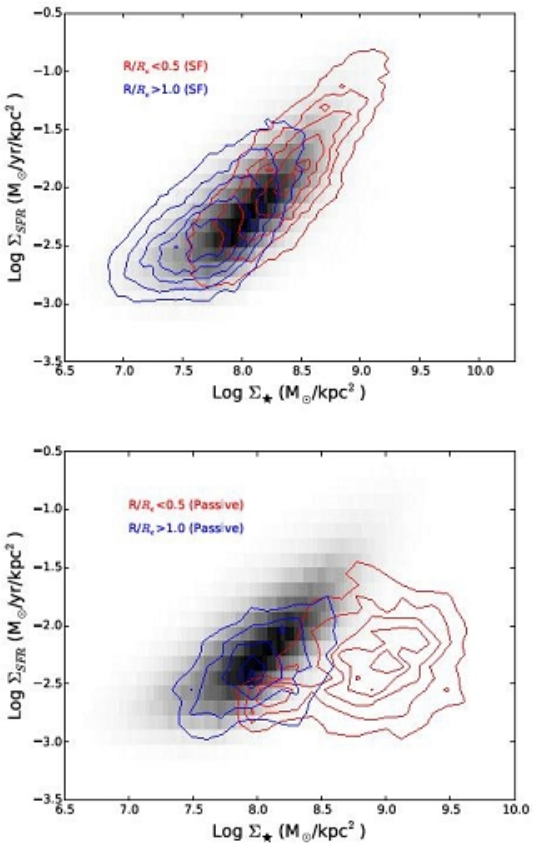

Figure 5. The grey histogram in both panels shows the resolved star forming main sequence for all star-forming spaxels (the sample shown in Fig. 4). Coloured contours show the distribution of $\Sigma_\star$ and $\Sigma_{\rm SFR}$ for star forming spaxels in star forming galaxies (top panel) and star forming spaxels in passive galaxies (bottom) panel in two bins of R/R_e. The most striking feature of this figure is the suppressed $\Sigma_{\rm SFR}$ values in passive galaxies at $R/R_e < 0.5$, indicating that quenching is most dramatic in the inner galactic regions, as expected from inside-out quenching.

Подавление – морфологический quenching?

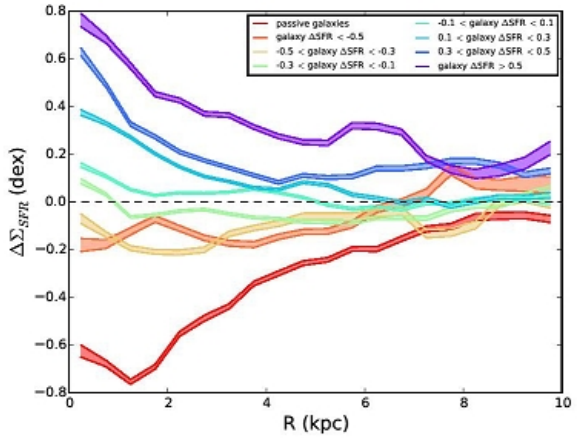

Figure 8. Radial profiles of $\Delta\Sigma_{SFR}$ for spaxels that inhabit galaxies with varying positions on the global main sequence (i.e. varying ΔSFR). The horizontal dashed line indicates zero enhancement or suppression of Σ_{SFR} relative to control spaxels of the same $\Sigma_\star$ and radial distance from the galaxy centre. The top and bottom panels show profiles on in units of R_e and kpc respectively.

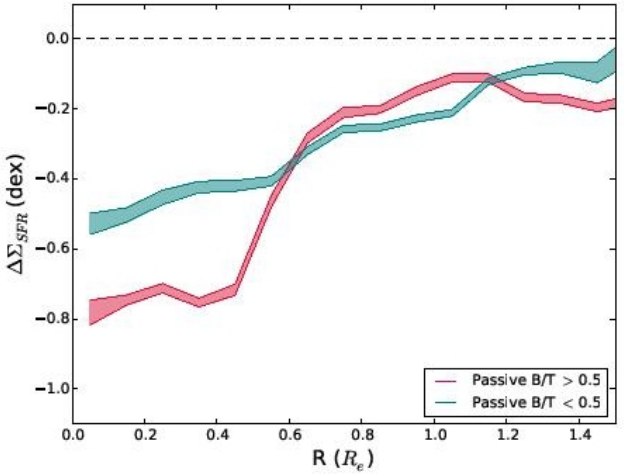

Figure 9. Radial profiles of $\Delta\Sigma_{SFR}$ for spaxels in disk dominated (teal line) and bulge dominated (crimson line) passive galaxies. Bulge fractions are determined from the bulge and disk mass catalog of Mendel et al. (2014). The horizontal dashed line indicates zero enhancement or suppression of Σ_{SFR} relative to control spaxels of the same $\Sigma_\star$ and radial distance from the galaxy centre.

А стимулирование SF inside-out – это аккреция металлобедного газа!

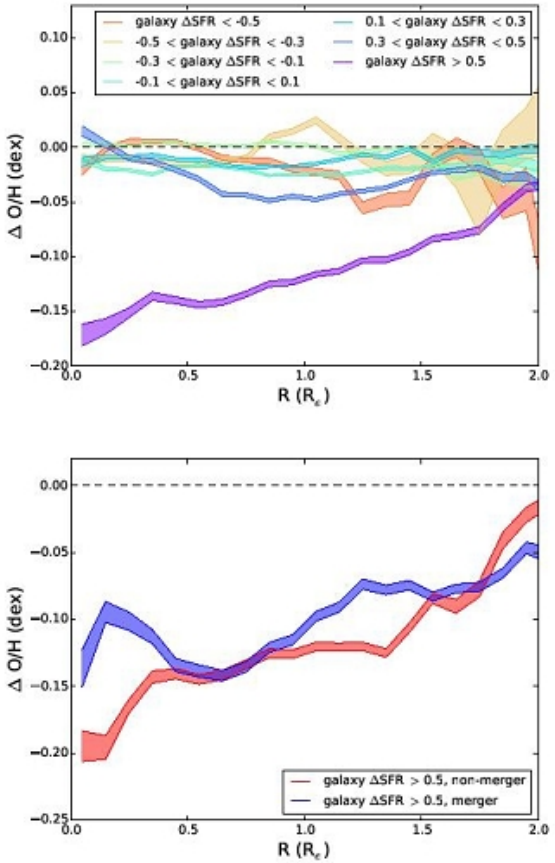

Figure 11. Top panel: Radial profiles of Δ O/H for spaxels that inhabit galaxies with varying positions on the global main sequence (i.e. varying ΔSFR). Bottom panel: Only galaxies in the highest ΔSFR bin (purple line in the top panel) separated into galaxies in likely mergers (either a close companion or obvious tidal disturbance) and non-mergers. The horizontal dashed line indicates zero enhancement or suppression of O/H relative to control spaxels of the same $\Sigma_\star$ and radial distance from the galaxy centre.

Astro-ph: 1711.02111

THE KMOS^{3D} SURVEY: ROTATING COMPACT STAR FORMING GALAXIES AND THE DECOMPOSITION OF INTEGRATED LINE WIDTHS †

E. WISNIOSKI[1], J. T. MENDEL[1], N. M. FÖRSTER SCHREIBER[1], R. GENZEL[1,2], D. WILMAN[3,1], S. WUYTS[4], S. BELLI[1], A. BEIFIORI[3,1], R. BENDER[3,1] G. BRAMMER[5], J. CHAN[6], R. I. DAVIES[1], R. L. DAVIES[1], M. FABRICIUS[1], M. FOSSATI[3,1], A. GALAMETZ[1], P. LANG[7], D. LUTZ[1], E. J. NELSON[1], I. MOMCHEVA[5], D. ROSARIO[8], R. SAGLIA[1], L. J. TACCONI[1], K. TADAKI[9], H. ÜBLER[1], P. G. VAN DOKKUM[10]

Draft version November 8, 2017

ABSTRACT

Using integral field spectroscopy we investigate the kinematic properties of 35 massive centrally-dense and compact star-forming galaxies ($\log(M_*[\mathrm{M}_\odot]) > 10$, $\log(\Sigma_{1\mathrm{kpc}}[\mathrm{M}_\odot\ \mathrm{kpc}^{-2}]) > 9.5$, $\log(M_*/r_e^{1.5}[\mathrm{M}_\odot\ \mathrm{kpc}^{-1.5}]) > 10.3$) at $z \sim 0.7-3.7$ within the KMOS^{3D} survey. We spatially resolve 23 compact star-forming galaxies (SFGs) and find that the majority are dominated by rotational motions with velocities ranging from $95-500$ km s^{-1}. The range of rotation velocities is reflected in a similar range of integrated Hα linewidths, $75-400$ km s^{-1}, consistent with the kinematic properties of mass-matched extended galaxies from the full KMOS^{3D} sample. The fraction of compact SFGs that are classified as 'rotation-dominated' or 'disk-like' also mirrors the fractions of the full KMOS^{3D} sample. We show that integrated line-of-sight gas velocity dispersions from KMOS^{3D} are best approximated by a linear combination of their rotation and turbulent velocities with a lesser but still significant contribution from galactic scale winds. The Hα exponential disk sizes of compact SFGs are on average 2.5 ± 0.2 kpc, $1-2\times$ the continuum sizes, in agreement with previous work. The compact SFGs have a $1.4\times$ higher AGN incidence than the full KMOS^{3D} sample at fixed stellar mass with average AGN fraction of 76%. Given their high and centrally concentrated stellar masses as well as stellar to dynamical mass ratios close to unity, the compact SFGs are likely to have low molecular gas fractions and to quench on a short time scale unless replenished with inflowing gas. The rotation in these compact systems suggests that their direct descendants are rotating passive galaxies.

Выборка – по центральной плотности (как у пассивных!)

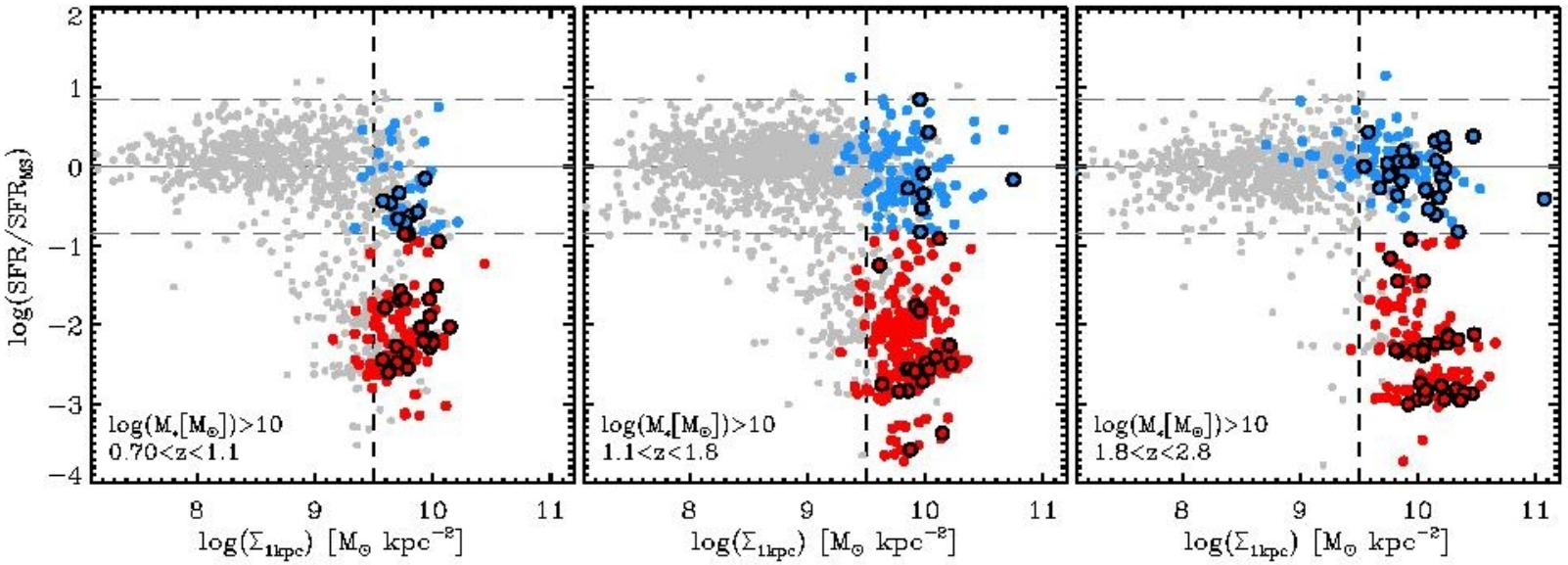

FIG. 1.— SFR/SFR$_{MS}$ vs. compactness, $\Sigma_{1.5}$ (top panels), and inner-kpc density, Σ_{1kpc} (bottom panels), as measured from HST H-band half light sizes for galaxies in v4.1.5 3D-HST/CANDELS which satisfy the KMOS^{3D} magnitude and visibility selection criteria. The three columns show the selection diagram in three redshift bins, $0.7 < z < 1.1$, $1.1 < z < 1.8$, and $1.8 < z < 2.8$. Blue circles are SFGs (ΔSFR> -0.85) with $\log(\Sigma_{1.5}) > 10.3$ and red circles are quiescent galaxies (ΔSFR< -0.85) with $\log(\Sigma_{1.5}) > 10.3$. Black open circles highlight galaxies already observed in KMOS^{3D}.

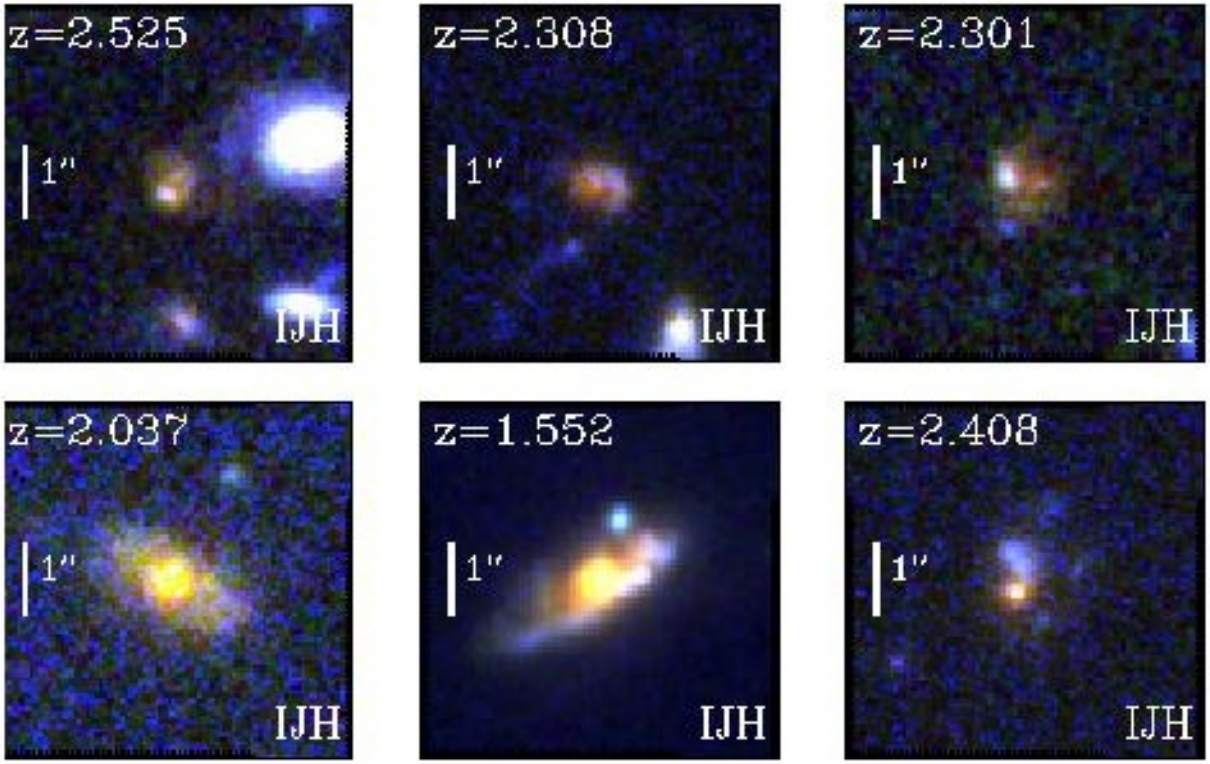

FIG. 2.— Example composite HST *IJH* images showing galaxies exclusively satisfying either the selection of compact galaxies ($\log(\Sigma_{1.5}[M_\odot\ \mathrm{kpc}^{-1.5})] > 10.3$; top) or of dense core galaxies ($\log(\Sigma_{1\mathrm{kpc}}[M_\odot\ \mathrm{kpc}^{-2}]) > 9.5$; bottom).

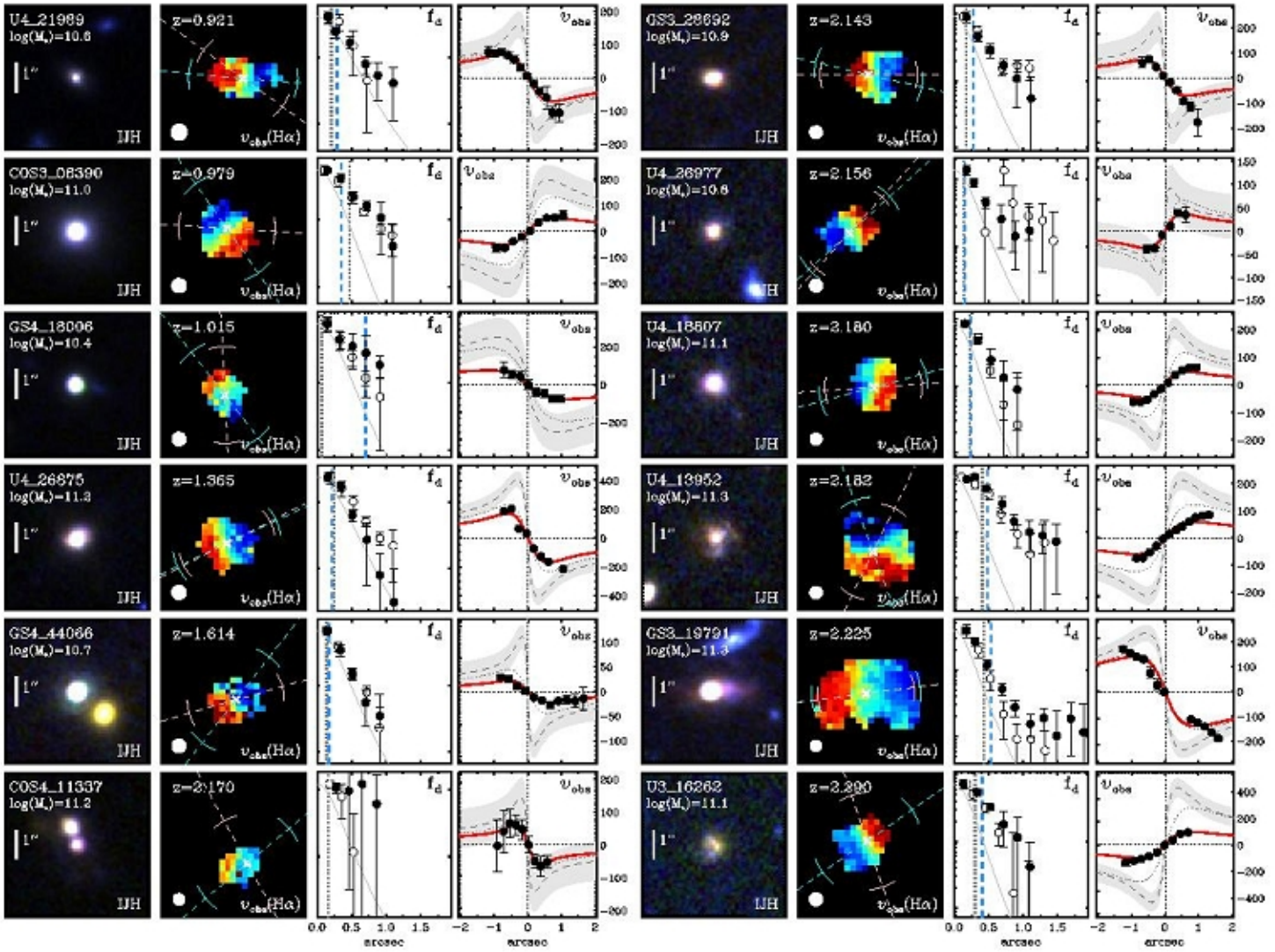

FIG. 5.— Extracted 2D and 1D kinematics of all resolved compact SFGs in our sample. From left to right: HST *IJH* color composite image; KMOS^{3D} Hα velocity map shown with FWHM of PSF specific to observations of this galaxy (white circle); normalized Hα emission (black points) profiles, normalized KMOS continuum (open points) and 1D PSF (gray line); observed Hα velocities along major kinematic axis (black points), fit with exponential disk model (red line). The axis profiles are extracted along the kinematic PA as denoted by the light blue line over plotted on the velocity map. The photometric PA, as determined by F160W HST images, is shown by the pink line. The blue arcs correspond to $\pm$18 degrees, the average misalignment between photometric and kinematic PAs, while the pink arcs correspond to $\pm 3\sigma$ error on the photometric PA. In the third panels the half-light radii measured from the *H*-band (dotted gray) and Hα maps (dashed blue) are shown by vertical lines. In the forth panels the dotted gray velocity curves show the best-ft exponential disk model with the inclination correction applied. The dashed gray velocity curve shows the intrinsic rotation curve. The associated shaded region shows the error on the rotational velocity, v_{corr}, corrected for both inclination and beam-smearing effects.

Нет места ни для темной материи, ни для большого количества газа!

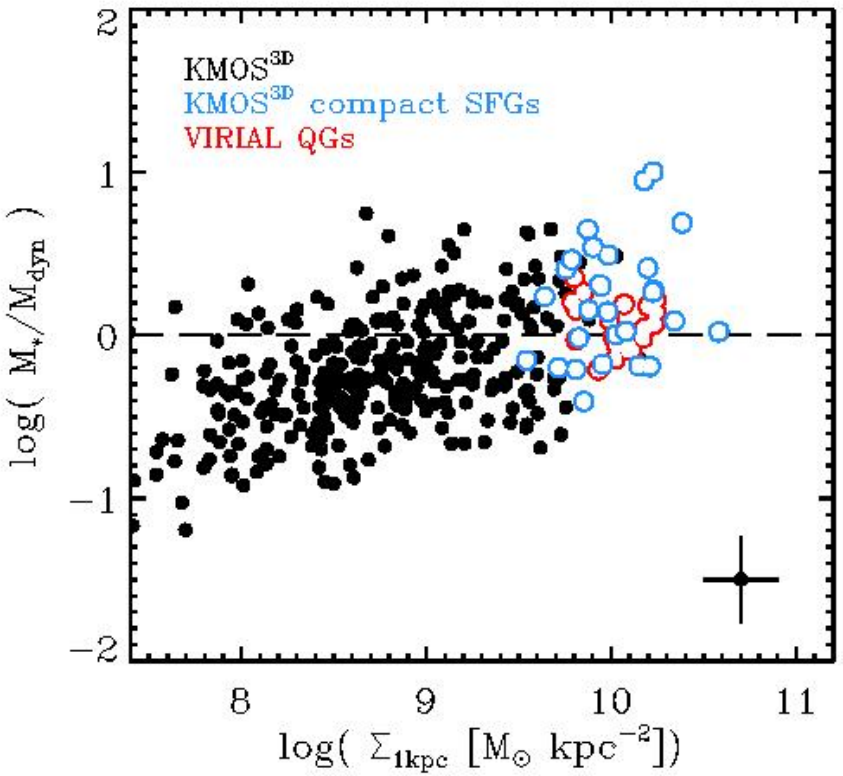

FIG. 9.— Stellar to dynamical mass fraction as a function of inner-kpc density for extended SFGs, compact SFGs, and quiescent galaxies (QGs). Dynamical masses are estimated from equation 3 for SFGs and from JAM modeling for quiescent galaxies from the VIRIAL survey (Mendel et al. 2015; *in prep*). A representative error 1-sigma bar is shown in the bottom right corner.

Nature Astronomy: Astro-ph: 1711.02336

Demise of Faint Satellites around Isolated Early-type Galaxies

Changbom Park[1], Ho Seong Hwang[2,*], Hyunbae Park[3], and Jong Chul Lee[3]

[1]School of Physics, Korea Institute for Advanced Study, Hoegiro 85, Seoul 02455, Korea

[2]Quantum Universe Center, Korea Institute for Advanced Study, Hoegiro 85, Seoul 02455, Korea; hhwang@kias.re.kr, *corresponding author

[3]Korea Astronomy and Space Science Institute, 776 Daedeokdae-ro, Yuseong-gu, Daejeon 34055, Korea

Выборка «изолированных» галактик ранних типов

Table 1. Isolated early-type host galaxies selected in this work.

NGC	RA[1]	DEC[1]	z	D[2]	m_r[3]	M_r	logM_*[4]	T	r_{vir}[5]	$m_{r,lim}$[6]	$M_{r,lim}$[7]	N_{sat}[8]
2592	126.78354	25.97031	0.006825	26.3	12.205	-20.05	10.60	E2	346	20.38	-11.71	7
3414	162.81754	27.97510	0.004903	25.7	10.918	-21.19	10.87	S0p	493	20.17	-11.87	9
3665	171.18196	38.76279	0.006835	33.1	10.786	-21.85	11.22	S0	604	20.17	-12.42	11
3872	176.45437	13.76668	0.010627	44.7	11.614	-21.77	11.30	E5	588	19.47	-13.77	10
4125	182.02453	65.17434	0.004523	24.0	10.258	-21.69	11.15	E	573	17.77	-14.11	6
5363	209.02998	5.25503	0.003799	13.6	10.283	-20.45	11.22	E/S0p	393	17.77	-12.90	15
5638	217.41823	3.23333	0.005591	26.5	11.178	-21.02	10.91	E1	468	20.09	-12.02	7

1. RA and DEC in degrees
2. Luminosity distances in units of Mpc.
3. Petrosian apparent magnitude in the r-band.
4. Stellar mass in units of $M_\odot$.
5. Virial radius in kpc.
6. Limiting magnitude where the completeness of the spectroscopic survey falls to 50%.
7. Limiting absolute magnitude corresponding to the limiting apparent magnitude.
8. Number of satellites identified in this work.

Наблюдения красных смещений всего, что вокруг

Supplementary Table 1. Spectroscopic survey of galaxies for five systems

Hosts	SDSS #	Trimester	Exposures(min)	N(z)[1]
NGC 2592	1142165	2016a	45/60/60/60	860
NGC 3414	2204882	2016a	45/60/60/60	897
NGC 3665	1317351	2014a	60/60	447
		2015b	60/60	508
NGC 3872	1122257	2016a	45/60	495
NGC 5638	485766	2015b	45/60/60/60	961
		2016a	60	144

1. The number of galaxy redshifts obtained newly.

Выбор спутников по фазовой диаграмме

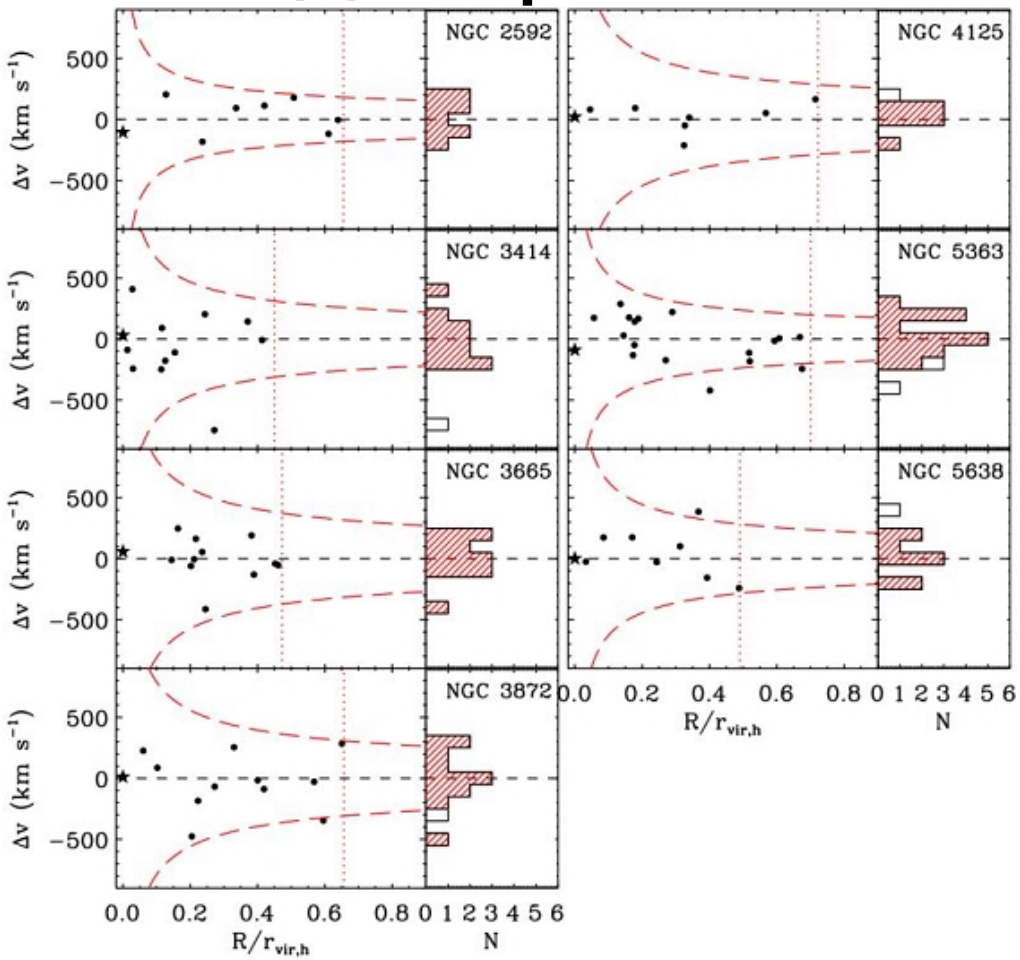

Supplementary Figure 2. The velocity difference with respect to the mean group velocity of the satellite system members as a function of host-centric distance and its histogram. The stars are the host galaxies, and points are satellite candidates. A typical

Общие свойства

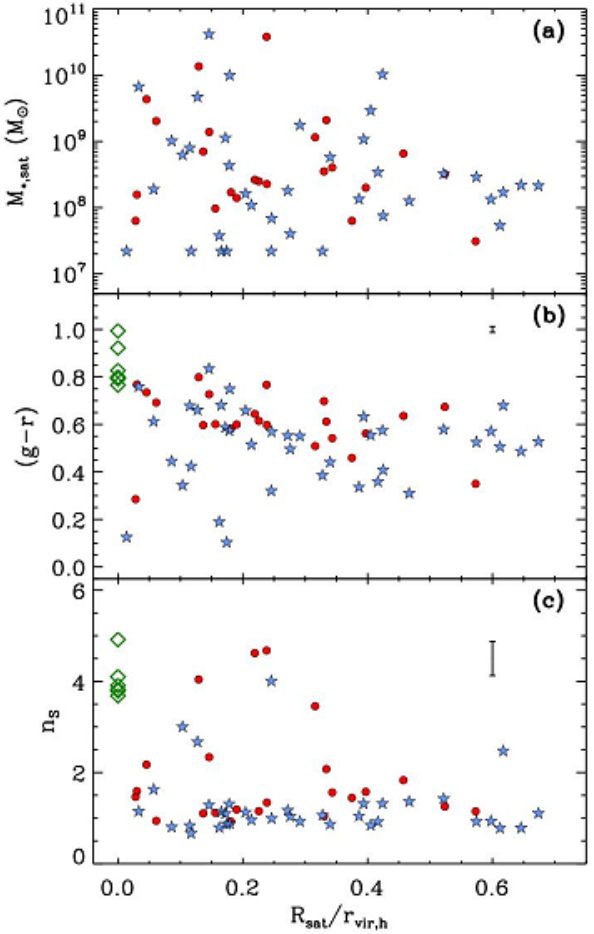

Figure 3. Physical parameters of galaxies in the seven satellite galaxy systems of Table 1 as a function of host-satellite distance in units of host virial radius. a, Stellar mass. **b,** g-r colour. **c,** Sérsic index. Red and blue symbols are early- and late-type satellites, respectively. Green diamonds represent host galaxies. Typical errors are represented with an error bar.

Функция светимости с обрывом…

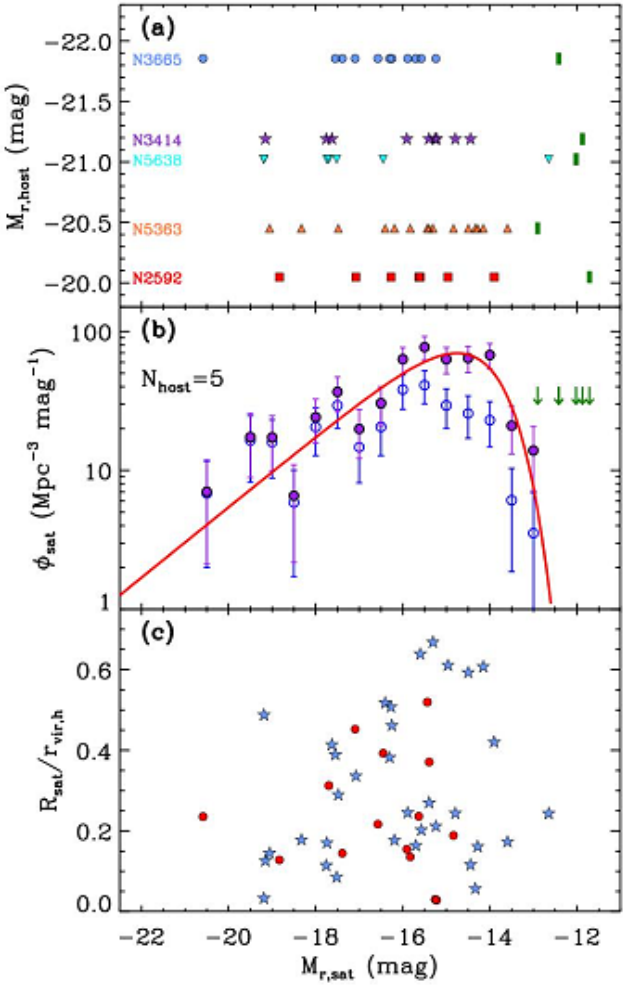

Figure 1. **Physical properties of satellite galaxies as a function of absolute magnitude. a,** Absolute magnitudes of host galaxies. The green vertical bars mark our survey limits in absolute magnitude for individual hosts. **b,** Luminosity function of the satellite galaxies in five systems (NGC 2592, NGC 3414, NGC 3665, NGC 5363, NGC 5638) showing a cutoff near M_r= -14. Open and filled circles are the functions before and after correction for the surface brightness incompleteness. The error bars correspond to the Poisson error. Vertical arrows mark

… не похожа на поле!

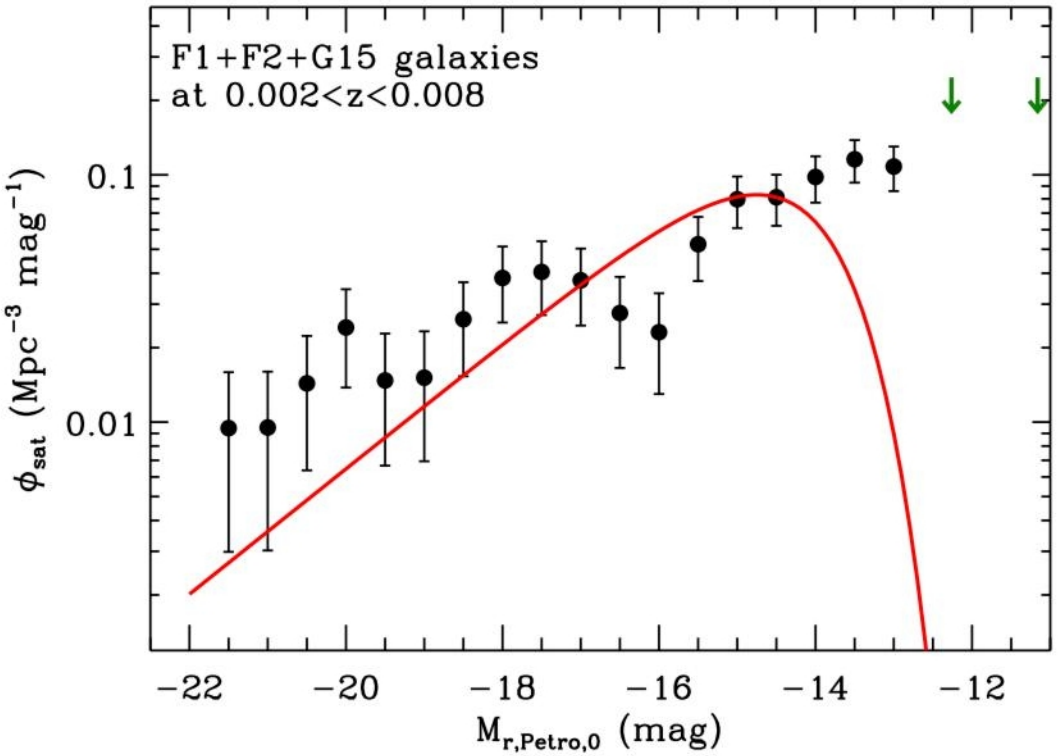

Figure 2. The luminosity function of the field galaxies in the GAMA G15 survey[19] and the SHELS F1 and F2 surveys[17,18]. The error bars correspond to the Poisson error. The left